

Determination of Near-Surface Anisotropy From Surface Electromagnetic Data

AbdulFattah Al-Dajani*, Frank Dale Morgan*, M. Nafi Toksöz*, and Philip Reppert†

Abstract

Ground penetrating radar (GPR) signatures, such as reflection moveout, are sensitive to the presence of azimuthal anisotropy. Azimuthal anisotropy can occur as an intrinsic property of the medium and/or due to the presence of fractures. In such cases, the GPR normal moveout (NMO) velocity, along different orientations of common-midpoint (CMP) gathers, varies with azimuth. This fact is well known in surface reflection seismology. The azimuthal variation of the NMO velocity in an arbitrary medium is elliptical. Considering the analogy between seismic wave propagation in surface seismology and GPR sounding, we can transfer some of the ideas between both fields, including the ellipticity of the NMO velocity in a fractured medium. Here, we discuss briefly GPR reflection moveout in azimuthally anisotropic media. Our study focuses on the transverse mode of electromagnetic wave propagation in which the polarization is normal to the incidence plane of the CMP gathers. A field data example is presented in which three GPR CMP gathers are acquired along three different azimuths, 60° apart, over a fractured medium. Our data analysis demonstrates the azimuthal variation of the GPR NMO velocity, which is utilized to invert for the local orientation of the fracture system in the near surface. The results obtained from the field example agree with the information obtained from geology and near surface studies. This work has important applications in imaging near surface geologic structures and in the determination of tectonic-induced fractures in the near surface.

1 Introduction

The application of ground penetrating radar (GPR) to fracture detection and anisotropy inversion in the near surface has not been utilized effectively by researchers. Recent studies and case histories in surface seismology, on the other hand, have shown that wave propagation signatures, including reflection moveout, are sensitive to the presence of azimuthal anisotropy. The complexity of the azimuthal anisotropy model depends on the type of fracture system that exists in the medium. Two of the most studied azimuthally anisotropic models are the horizontal transverse isotropy (HTI) and the orthorhombic models. An HTI model may occur due to the presence of a vertical, single-fracture system in an isotropic matrix. An orthorhombic model, on the other hand, may result from the presence of two orthogonal fracture systems in an isotropic matrix or from the presence of a single vertical fracture system in an anisotropic matrix (Figure 1). Fortunately, the analogy between surface seismic and GPR (McCann et al. (1988)), and contributions such as those by Annan and Cosway (1992), Reppert et al. (1998), Reppert et al. (1999), Cist (1999), Grechka and Tsvankin (1998), Al-Dajani and Tsvankin (1998), Al-Dajani and Toksöz (1999), and Al-Dajani and Toksöz (2000), allow us to transfer some of the technology from surface seismic to GPR.

The azimuthal dependence of seismic reflection moveout and the normal moveout (NMO) velocity in azimuthally anisotropic media have been discussed in detail by Grechka and Tsvankin (1998), Grechka et al. (1997), Al-Dajani and Tsvankin (1998), Al-Dajani and Toksöz (1999), Al-Dajani and Toksöz (2000), Al-Dajani et al. (1999), and Al-Dajani and Alkhalifah (2000). Despite the complexity of the azimuthal anisotropy in the medium, the NMO velocity for surface seismology has a relatively simple azimuthal variation

*Earth Resources Laboratory, Department of Earth, Atmospheric and Planetary Sciences, Massachusetts Institute of Technology, 42 Carleton st., Bldg E34, Cambridge, MA 02142.

†Formerly, Earth Resources Laboratory, Department of Earth, Atmospheric and Planetary Sciences, Massachusetts Institute of Technology. Now, Clemson University, South Carolina.

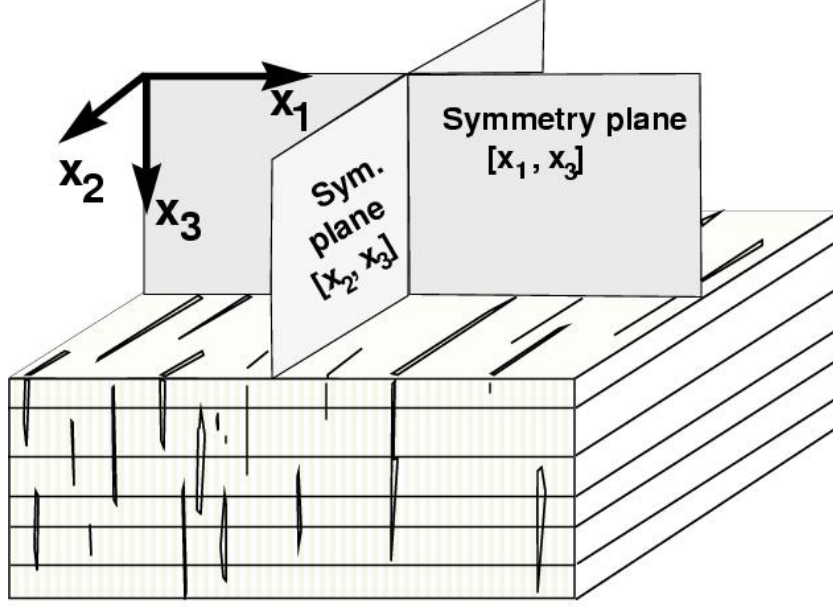


Figure 1: Orthorhombic media have three mutually orthogonal planes of mirror symmetry. One of the reasons for orthorhombic anisotropy is a combination of parallel vertical cracks and vertical transverse isotropy (e.g., due to thin horizontal layering) in the background medium, after [Grechka and Tsvankin \(1998\)](#).

with azimuth. Here, we focus our attention toward the reflection moveout for GPR in azimuthally anisotropic media. We describe the azimuthal behavior of the normal-moveout (NMO) velocity for GPR reflections. In principle, the key difference between GPR and surface seismic is the interpretation of the NMO velocity and how it relates to the medium. The NMO velocity from seismic data allows for the estimation of elastic constants, while the NMO velocity from GPR data allows the estimation of dielectric constants [see [McCann et al. \(1988\)](#), [Al-Dajani and Tsvankin \(1998\)](#), [Al-Dajani and Toksöz \(1999\)](#), and [Al-Dajani and Toksöz \(2000\)](#)]. Finally, we present a field data example to demonstrate the application of the azimuthal variation of the GPR NMO velocity to invert for the medium parameters (i.e., the detection and characterization of the local fracture system).

2 Mathematical Foundation in Reflection Moveout in Anisotropic Media

The 3-D fundamental equations of electromagnetic (EM) wave theory are given by Maxwell's equations:

$$\begin{aligned} -\nabla \times \mathbf{E} &= \mu \cdot \frac{\partial \mathbf{H}}{\partial t} \\ \nabla \times \mathbf{H} &= \epsilon \cdot \frac{\partial \mathbf{E}}{\partial t} + \mathbf{J}_c + \mathbf{J}_s, \end{aligned} \quad (1)$$

where \mathbf{E} and \mathbf{H} are the electric and magnetic fields. \mathbf{J}_c and \mathbf{J}_s are the conductive and source current, while ϵ and μ are the permittivity and permeability tensors:

$$\epsilon = \begin{pmatrix} \epsilon_{11} & 0 & 0 \\ 0 & \epsilon_{22} & 0 \\ 0 & 0 & \epsilon_{33} \end{pmatrix}, \text{ and}$$

$$\mu = \begin{pmatrix} \mu_{11} & 0 & 0 \\ 0 & \mu_{22} & 0 \\ 0 & 0 & \mu_{33} \end{pmatrix}.$$

We should mention that in the case of isotropy both ϵ and μ reduce to scalar quantities. The theory of GPR wave propagation is discussed in detail in many classic textbooks and in the literature (e.g., [Auld \(1990\)](#); and [Kong \(1990\)](#)), in which equation (1) is used to describe EM wave propagation theory. Here, we are interested in the concept of the kinematics of reflection moveout for GPR.

2.1 Reflection Moveout in Anisotropic Media

Reflection moveout for offsets (i.e., distances) less than or equal to the target depth is well approximated by the well-known hyperbolic reflection moveout equation:

$$t^2 = t_0^2 + A_2(\alpha)x^2, \quad (2)$$

where t_0 is the zero-offset reflection time, x is the source-receiver offset, and $A_2(\alpha)$ is the quadratic coefficient:

$$A_2 = \frac{1}{V_{\text{nmo}}^2(\alpha)}.$$

Here, $V_{\text{nmo}}(\alpha)$ is the normal-moveout velocity along an azimuth α defined as

$$V_{\text{nmo}}^2(\alpha) = \lim_{x \rightarrow 0} \frac{d(x^2)}{d(t^2)}, \quad (3)$$

and α is the azimuth of the CMP line.

To obtain the quadratic A_2 coefficient of the Taylor series expansion of the squared traveltime $[t^2(x^2)]$, we first find an expression for the coefficients in terms of the one-way traveltime from the zero-offset reflection point. For simplicity, we consider the case of an azimuthally anisotropic medium with a horizontal interface. Since a horizontal reflector that coincides with a symmetry plane represents a mirror image, the group-velocity (ray) vector of any pure (non-converted) reflected wave represents a mirror image of the incident ray with respect to the horizontal plane ([Al-Dajani and Tsvankin \(1998\)](#)). Thus, there is no reflection-point dispersal on CMP gathers above a homogeneous anisotropic layer with a horizontal symmetry plane. We can now represent the two-way traveltime along the specular ray path as the sum of the traveltimes from the zero-offset reflection point to the source and receiver (Figure 2). Following the approach suggested by [Hale et al. \(1992\)](#) in their derivation of the normal-moveout velocity from dipping reflectors, the one-way traveltime from the reflection point to the source or receiver can be expanded in a double Taylor series in the vicinity of the zero-offset point (see [Al-Dajani and Toksöz \(1999\)](#) and [Grechka and Tsvankin \(1998\)](#)). Here, we are particularly interested in deriving the quadratic moveout coefficient, so we keep the quadratic and lower-order terms in the Taylor series,

$$\tau(\pm x_1, \pm x_2) = \sum_{l=0}^2 \frac{D_{\pm x_1, \pm x_2}^l \tau}{l!}, \quad (4)$$

where

$$D_{\pm x_1, \pm x_2}^l \tau = \sum_{i+j=l} \frac{l!}{i!j!} (\pm x_1)^i (\pm x_2)^j \left(\frac{\partial}{\partial x_1}\right)^i \left(\frac{\partial}{\partial x_2}\right)^j \tau.$$

τ is the one way traveltime and $(\pm x_1, \pm x_2)$ correspond to the coordinates of the source (+) and receiver (-) in the vicinity of the common-midpoint (CMP) location (O) (see Figure 2). The derivatives are evaluated at the CMP location.

As a result, the two-way traveltime (t) is given as:

$$t = \tau_+ + \tau_-, \quad (5)$$

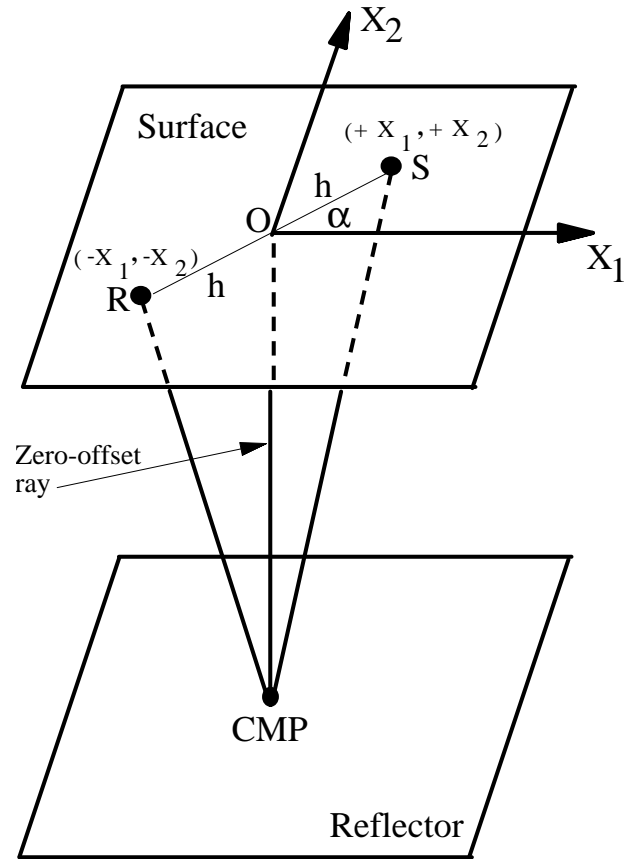


Figure 2: For a homogeneous azimuthally anisotropic layer with a horizontal symmetry plane, the specular reflection point for any offset coincides with the zero-offset reflection point, and there is no reflection-point dispersal on CMP gathers. h is half the offset between the source (S) and the receiver (R), and the angle α is the azimuth of the CMP gather from the x_1 axis.

where $\tau_+ \equiv \tau(+x_1, +x_2)$ is the one-way time from the source (S) to the CMP location, while $\tau_- \equiv \tau(-x_1, -x_2)$ is the one-way traveltime from the CMP location back to the receiver (R) (Figure 2).

Substituting equation (4) into equation (5), the two-way traveltime is given by:

$$t = 2\tau_0 + x_1^2\tau_{11} + 2x_1x_2\tau_{12} + x_2^2\tau_{22}, \quad (6)$$

where τ_0 is the one-way zero-offset time and $\tau_{ij} = \frac{\partial^2\tau}{\partial x_i\partial x_j}$. The indices i and j take the values 1 and 2 corresponding to the Cartesian coordinates x_1 and x_2 , respectively.

The coordinates x_1 and x_2 can be expressed in terms of the azimuth α and the half offset h of the CMP line, as demonstrated in Figure 2:

$$\begin{aligned} x_1 &= h \cos \alpha, \\ x_2 &= h \sin \alpha. \end{aligned} \quad (7)$$

Substituting equation (7) into equation (6) and squaring both sides of equation (6), we obtain (after simplification and keeping only the quadratic and lower-order terms):

$$t^2 = t_0^2 + A_2(2h)^2, \quad (8)$$

where

$$A_2 = \frac{t_0}{2}(\tau_{11} \cos^2 \alpha + 2\tau_{12} \sin \alpha \cos \alpha + \tau_{22} \sin^2 \alpha), \quad (9)$$

where t_0 is the two-way zero-offset time, and α is the angle between the CMP line and one of the principal vertical planes [in this case, we have chosen the (x_1, x_3) plane to be our reference plane].

For a more convenient notation, let us rewrite the coefficients in equation (9) as follows:

$$\begin{aligned} A_2(\alpha) &= A_2^{(1)} \sin^2 \alpha + A_2^{(2)} \cos^2 \alpha \\ &+ A_2^{(x)} \sin \alpha \cos \alpha, \end{aligned} \quad (10)$$

where α is, again, the angle between the CMP line and one of the principal vertical planes [e.g., (x_1, x_3) plane]. The superscripts (1) and (2) are the components of the coefficient along the two vertical principal planes [in Cartesian coordinates, (x_2, x_3) and (x_1, x_3) , respectively]. The superscript (x) is used to represent the cross term that absorbs the mutual influence from all principal planes. The components of the coefficients are presented in terms of the medium parameters, while the azimuthal dependence is governed by the trigonometric functions. Equation (10) is identical to the equation that was introduced by Grechka and Tsvankin (1998) to describe the NMO velocity in azimuthally anisotropic media for pure modes of seismic wave propagation. Here, we use equation (10) as a basis for our study of the NMO velocity for GPR reflection moveout in anisotropic media.

It is important to mention that equation (10) is a general representation of an ellipse, in which $A_2^{(1)}$ and $A_2^{(2)}$ are the semi-axes of the ellipse, and $A_2^{(x)}$ controls the orientation of the ellipse. We should mention that for any horizontal, azimuthally anisotropic medium with a horizontal symmetry plane (e.g., horizontal transverse isotropy and orthorhombic), $A_2^{(x)} = 0$, assuming that the symmetry planes of the medium coincides with the Cartesian coordinate system. Moreover, equation (10) is not only restricted to a medium with a horizontal interface, but is also valid for any arbitrary medium (for more details, see Grechka and Tsvankin (1998)).

Figure 3 shows a schematic diagram for the azimuthal variation of the quadratic coefficient A_2 and its inverse (the square of the NMO velocity). Note that Figures 3a, b correspond to the case of an arbitrary medium, while Figures 3c, d correspond to an azimuthally anisotropic medium with horizontal reflector and symmetry plane (e.g., HTI and orthorhombic). As seen in Figures 3b, d, the azimuthal variation of the NMO velocity in azimuthally anisotropic media is elliptical.

We emphasize that no assumptions are made in the above derivation regarding the anisotropic (or the medium) model, the type of wave, the wave mode, and the strength of anisotropy. Therefore, despite the fact that the above discussion was originally designed for surface seismology, it is still valid for GPR reflections. The key issue is to find the proper interpretation of the NMO velocity in terms of the medium parameters.

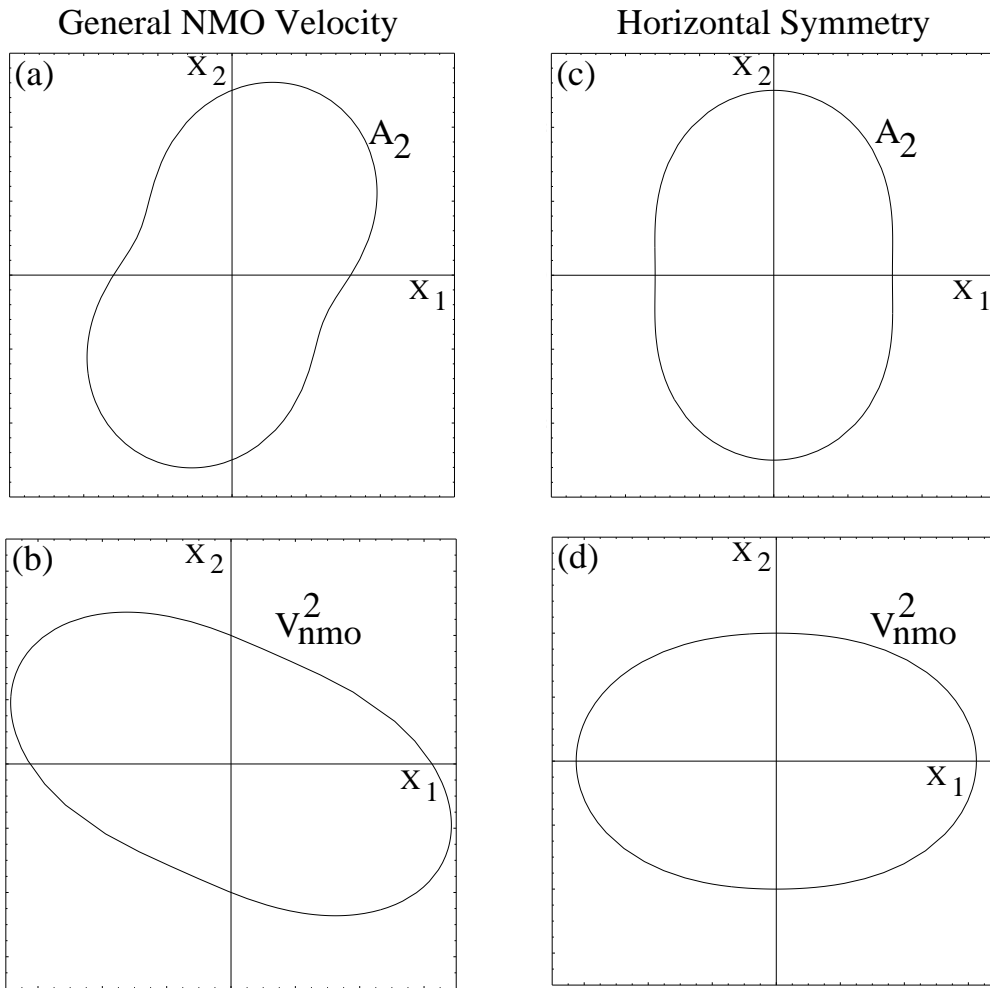


Figure 3: A plan view of the general behavior of the quadratic coefficient (A_2) and its inverse (V_{nmo}^2) for GPR wave propagation in an arbitrary medium (a and b), and in an orthorhomic medium with a horizontal reflector (c and d).

2.2 GPR Normal Moveout (NMO) Velocity

The GPR normal moveout (stacking) velocity, V_{nmo} , for an azimuthally anisotropic medium is given, in general, as an ellipse:

$$V_{\text{nmo}}^2(\alpha) = \frac{V_{\text{nmo},1}^2 V_{\text{nmo},2}^2}{V_{\text{nmo},1}^2 \cos^2(\alpha - \beta) + V_{\text{nmo},2}^2 \sin^2(\alpha - \beta)}, \quad (11)$$

where the semi-axes of the NMO ellipse, $V_{\text{nmo},1}^2 \equiv \frac{1}{A_2^{(1)}}$ and $V_{\text{nmo},2}^2 \equiv \frac{1}{A_2^{(2)}}$, are the NMO velocities along the two vertical principal planes, respectively. α is the azimuth of the CMP gather relative to the principal direction, β , where here we assume that $\beta = 0$ (i.e., the vertical symmetry planes are aligned with the coordinate system).

Our goal is to implement equation (11) to GPR reflection moveout. We consider the transverse mode of GPR wave propagation (i.e., the polarization is perpendicular to the incidence plane). In this case, $V_{\text{nmo},1} = \frac{c}{\sqrt{\epsilon_1 \mu_1}}$ and $V_{\text{nmo},2} = \frac{c}{\sqrt{\epsilon_2 \mu_2}}$ (see Auld (1990)), where $c = 3 \times 10^8$ m/s, while ϵ_1 and ϵ_2 are the relative dielectric constants along the vertical principal directions and parallel to the polarization. μ_1 and μ_2 , on the other hand, are the relative magnetic permeabilities along the principal directions. In the case of nonmagnetic strata, as is the case in our field example below, $\mu_1 = \mu_2 = \mu = 1$. It is obvious that the direction of the major semi-axis is the direction of the fastest velocity (e.g., parallel to the fracture), while the direction of the minor semi-axis is the direction of the slowest velocity (e.g., perpendicular to the fracture). Analogous expressions can be obtained for other modes of EM wave propagation.

The strength of azimuthal anisotropy can be obtained as:

$$\text{Anisotropy}_{\text{strength}} = 100 \frac{V_{\text{nmo},1} - V_{\text{nmo},2}}{V_{\text{nmo},1}}. \quad (12)$$

2.3 GPR NMO Velocity in Multilayered Media

In multilayered anisotropic media the quadratic moveout coefficient reflects the combined influence of layering and anisotropy. For conventional spreadlength-to-depth ratios (i.e., ≤ 1), the hyperbolic moveout equation (2) can be expected to provide an adequate description of the moveout, but the NMO velocity should be averaged over the stack of layers. In isotropic and vertical transverse isotropic (VTI) media, this averaging is performed by using the conventional isotropic Dix (1955) equation (Hake et al. (1984)):

$$V_{\text{nmo}}^2 = \frac{1}{t_0} \sum_i^N V_{2i}^2 \Delta t_i, \quad (13)$$

where t_0 is the two-way zero-offset time to reflector N , V_{2i} is the NMO velocity for each individual layer i , and Δt_i is the two-way zero-offset time in layer i .

In addition, Alkhalifah and Tsvankin (1995) showed that the Dix equation remains valid in symmetry planes of any anisotropic medium, if the interval NMO velocities are evaluated at the ray-parameter value of the zero-offset ray. A more general Dix-type equation, that properly accounts for both azimuthal anisotropy and vertical inhomogeneity, was recently developed by Grechka et al. (1997) for arbitrary media:

$$\mathbf{W}^{-1}(L) = \frac{1}{\tau(L)} \sum_{\ell=1}^L \tau_{\ell} \mathbf{W}_{\ell}^{-1}, \quad (14)$$

where \mathbf{W}_{ℓ} are interval matrices, or equivalently, interval NMO velocities, given as ellipses. Traveltimes τ_{ℓ} should be obtained from the kinematic ray tracing (i.e., by computing group velocity) of the zero-offset ray. Equation (14) performs Dix-type averaging of the interval matrices \mathbf{W}_{ℓ} to obtain the effective matrix $\mathbf{W}(L)$ [i.e., the effective normal-moveout velocity $V_{\text{nmo}}(\alpha, L)$]. Note that the effective NMO velocity is also an ellipse (for more discussion, see Grechka et al. (1997)). Along the vertical symmetry planes, equation (14) reduces to the well-known conventional Dix (1955) equation (13). The interval NMO velocity for any wave type in arbitrary anisotropic media is given by equation (10). For anisotropic media with horizontal symmetry

planes (e.g., HTI or orthorhombic media) and horizontal interfaces, the interval NMO velocity is given by equation (11). We should mention that equation (13) is exact along the symmetry planes in azimuthally anisotropic media. Outside the symmetry planes, however, equation (13) is an approximation with excellent accuracy (Al-Dajani and Toksöz (1999); Al-Dajani and Tsvankin (1998)).

3 Field Data Example

Al-Dajani et al. (1999) have shown that to utilize the elliptical variation of the NMO velocity, and to obtain an optimum inversion result for the NMO ellipse, at least three CMP gathers, 60° apart, are needed. As a result, in our data collection we made use of this conclusion in which we have collected three GPR CMP gathers, 60° apart, over a fractured nonmagnetic medium. We will utilize the azimuthal variation of the GPR NMO velocity to invert for the NMO ellipse. Hence, the local fracture system, characterized by the semi-axes and orientation of the NMO ellipse, can be obtained.

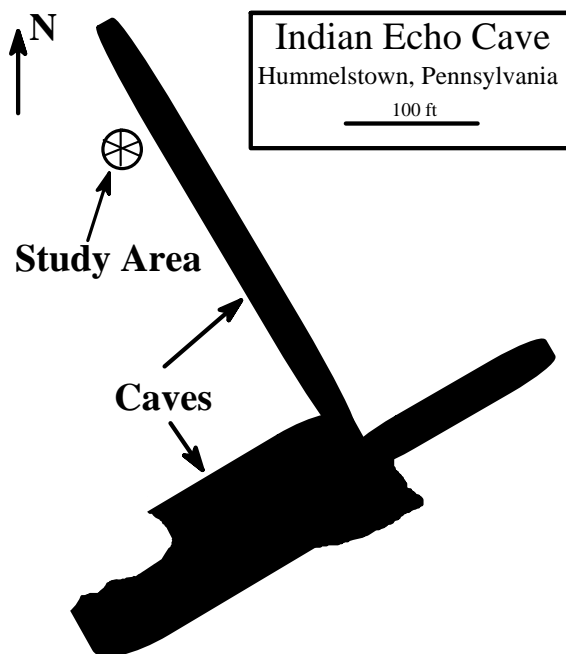


Figure 4: Sketch map for the location of the study area relative to the cave system. The map is simplified from its original form that was created by the York Grotto of the National Speleological Society.

3.1 Data Collection

Data were collected at the Indian Echo Caverns, about 10 miles east of Harrisburg, Pennsylvania. A Pulse Echo IV Radar system was used with 50 MHz antennas. The data were collected in perpendicular broadside configuration in which the EM wave is polarized normal to the incidence plane of the CMP gather. Indian Echo Caverns consists of a two cave system running perpendicular to each other in Beekmantown Limestone. Figure 4 shows a location map of the study area relative to the cave system. Three CMP gathers were collected along three different azimuths: 60° ($\equiv 240^\circ$) for CMP 1, 120° (300°) for CMP 2, and 0° (180°) for CMP 3, measured relative to the geographic north (Figure 5).

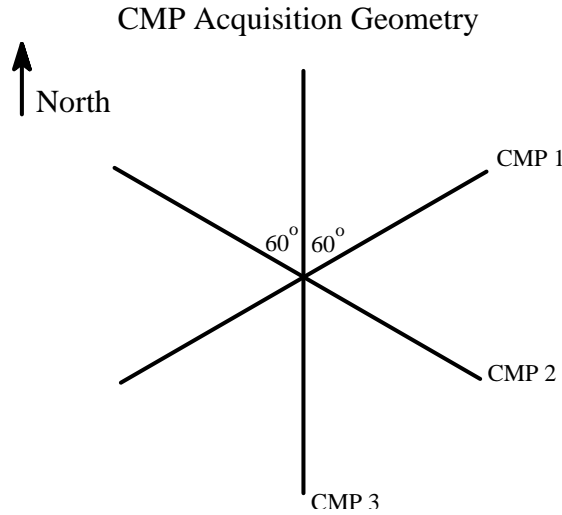


Figure 5: A plan view of the acquisition geometry for the three CMP gathers along azimuths: 60° ($\equiv 240^\circ$) for CMP 1, 120° (300°) for CMP 2, and 0° (180°) for CMP 3, measured relative to the geographic north.

3.2 Data Processing and Results

Standard processing steps were applied to the CMP gathers (e.g., [Yilmaz \(1987\)](#); [Annan and Cosway \(1992\)](#)), using the Seismic Unix (SU) software. The processing steps include:

- Automatic Gain Control (AGC)
- Spiking Deconvolution (DEC)
- Band Pass Filter (BPF)
- Dip Filter (DPF)
- Velocity analysis (VELAN)
- NMO correction (NMO)
- Mute (MUT)

Figures 6-8 show the three CMP gathers in their raw form (after applying AGC) and in their processed form (after applying the complete processing scheme shown above). A careful velocity analysis has been conducted to extract accurate NMO-velocity functions for the three CMP gathers. The accuracy of the NMO velocity functions for the CMPs are demonstrated by the alignments of the reflections after moveout correction (Figures 6-8). Figure 9 shows the three velocity-function profiles along the three azimuths. It is clear that the GPR velocity functions vary with azimuth. Note, however, that the sensitivity of NMO velocity estimation for reflections below 3.510^{-7} seconds (350 nanoseconds) deteriorates which makes the inversion unreliable below that point.

By applying a nonlinear inversion to estimate the best fit ellipse to the three NMO-velocity profiles of Figure 9 ([Al-Dajani et al. \(1999\)](#)), we obtain the semi-axes (major and minor) of the NMO ellipse, the ellipse orientation, and the strength of azimuthal anisotropy as given by equation (12). The results of this inversion are shown in Figure 10. As shown in Figure 10, the azimuthal anisotropy strength, given in percent, in the NMO (stacking) velocity ranges from 5 to 25% with an average value of about 10% in the near surface. The orientation of the NMO ellipse, on the other hand, ranges from -10° (350°) to -35° (325°) with an average

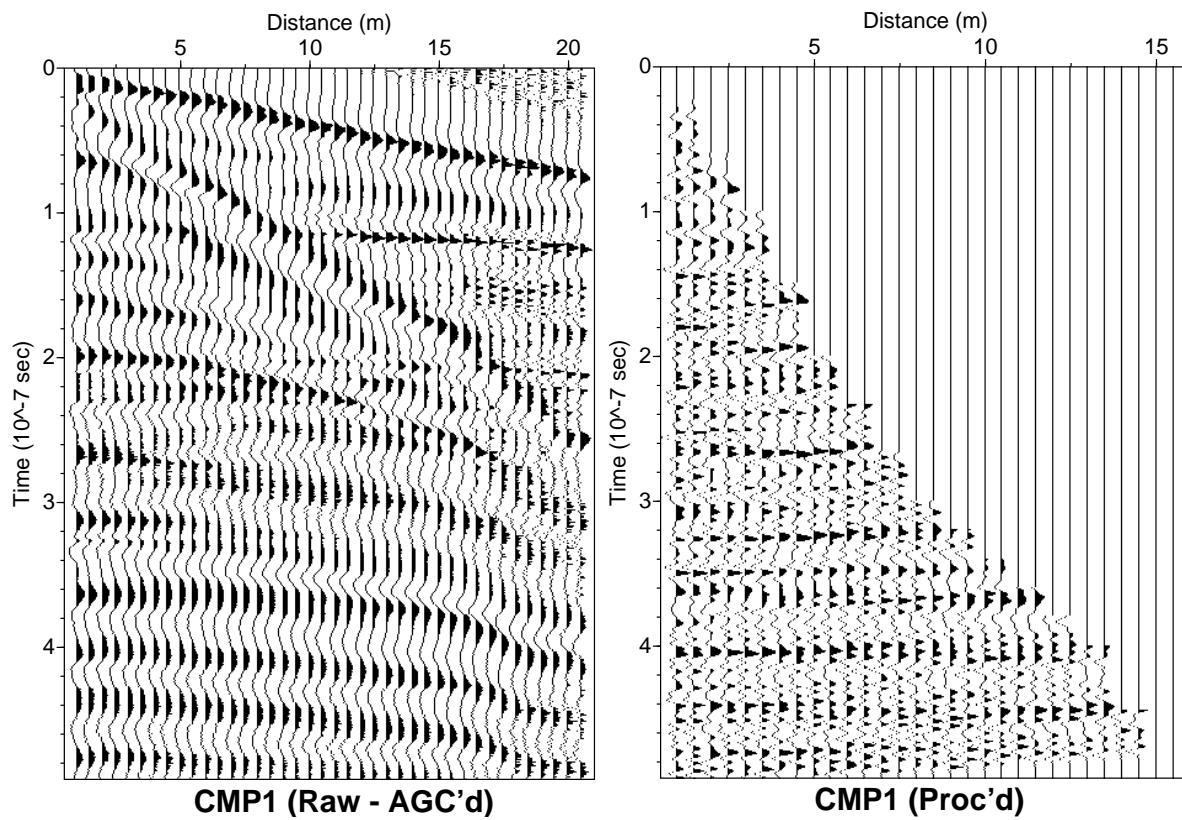


Figure 6: Comparison between raw data (after applying AGC) and processed data (after applying the complete processing flow) for CMP 1. Figure 5 shows the acquisition geometry for the CMP gather.

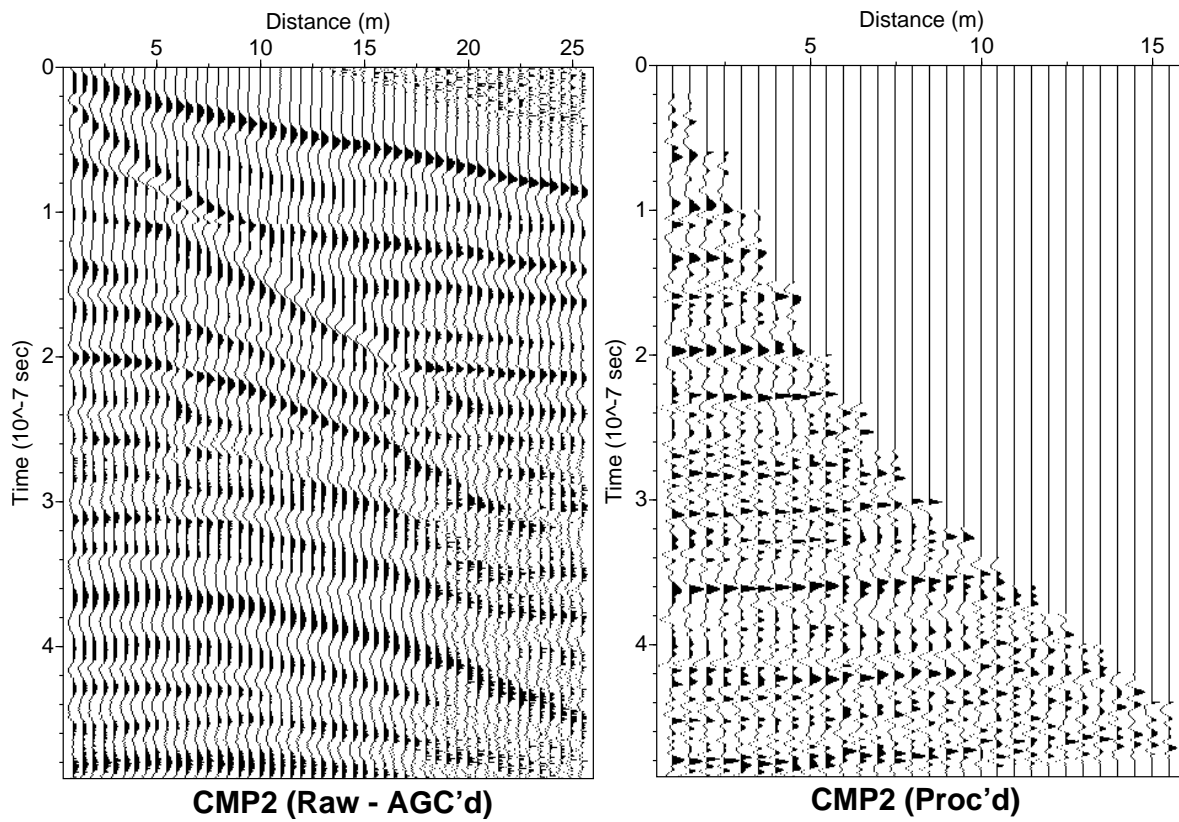


Figure 7: Comparison between raw data (after applying AGC) and processed data (after applying the complete processing flow) for CMP 2. Figure 5 shows the acquisition geometry for the CMP gather.

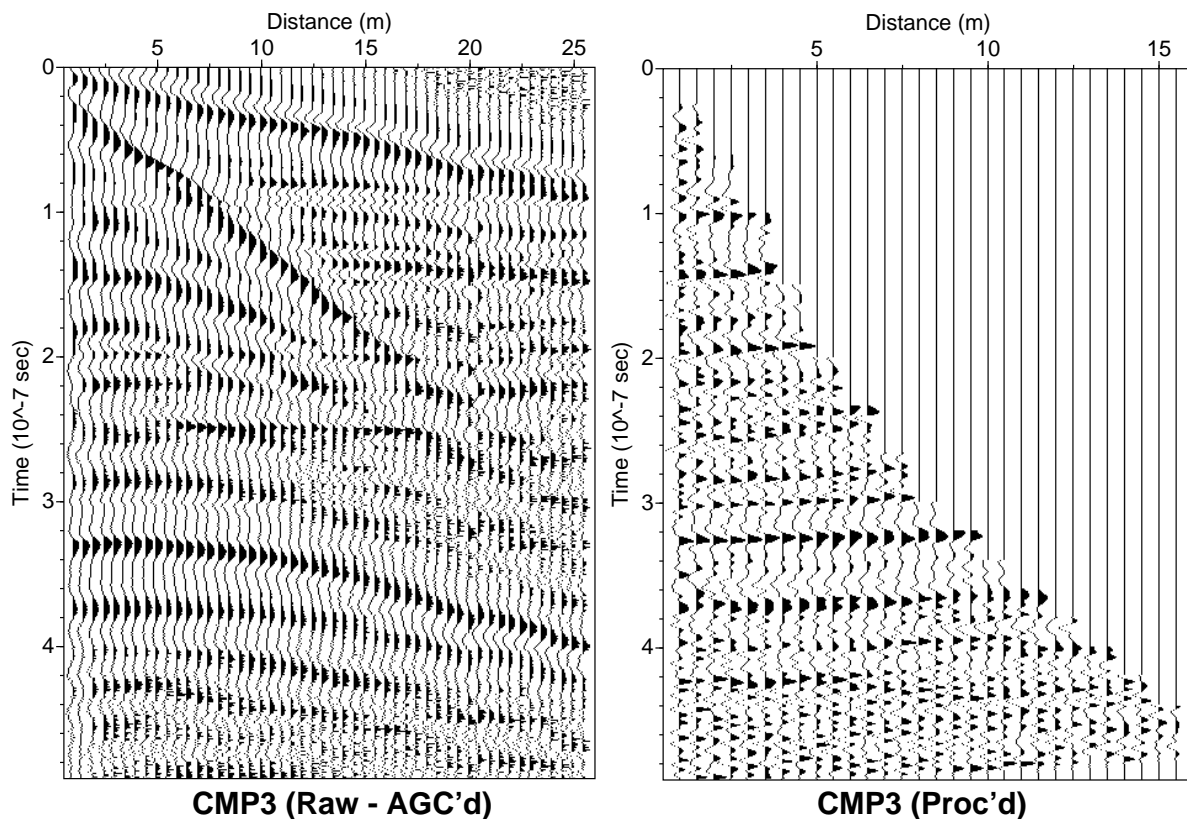


Figure 8: Comparison between raw data (after applying AGC) and processed data (after applying the complete processing flow) for CMP 3. Figure 5 shows the acquisition geometry for the CMP gather.

orientation of about -30° (330°), relative to the geographic north (Figure 10). It is interesting to note that the orientation of the NMO ellipse coincides with the local fracture system (i.e., stress field) as it manifests itself in the development of the local cave system in the vicinity of the study area (Figure 11). Applying Dix-type differentiation to the NMO-velocity ellipses allows the estimation of the interval velocity anisotropy; hence, the characterization of zones of special interest. In order to perform such inversion with confidence, however, we need more NMO velocity measurements (see Al-Dajani et al. (1999)) and it is beyond the scope of this study.

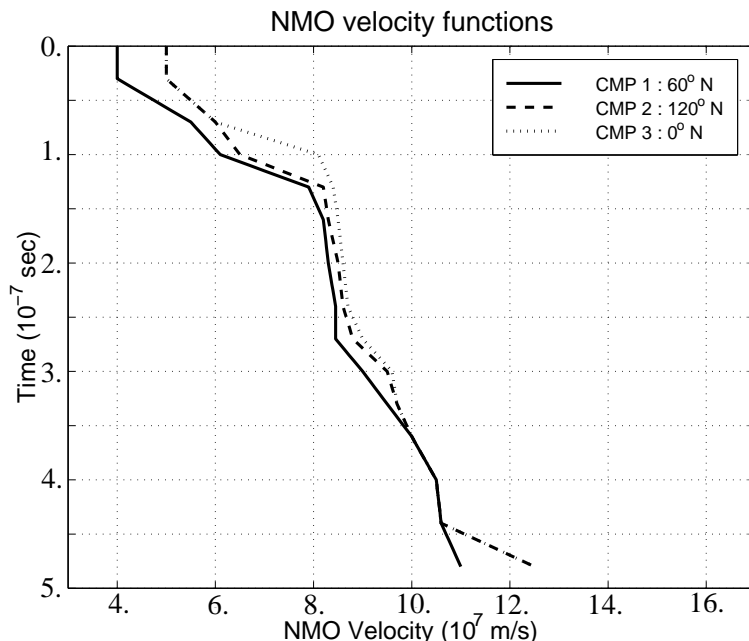


Figure 9: NMO (stacking) velocity functions for the three CMP gathers, resulting from the VELAN process.

4 Discussion and Conclusion

We have discussed GPR reflection moveout in azimuthally anisotropic media. We demonstrated that the NMO velocity for GPR reflection moveout for azimuthally anisotropic medium is elliptical, analogous to the case of surface seismology. The azimuthal variation of the GPR NMO velocity is demonstrated by a real data example. We conducted an experiment where three GPR CMP gathers were acquired along three different azimuths, 60° apart, over a fractured medium. The transverse component (perpendicular polarization, relative to the incident plane) was collected for this study. Our GPR data analysis was utilized successfully to invert for the principal directions of a fractured medium. The results show that the azimuthal variation of the GPR NMO velocity allows the inversion for the local orientation of the fracture system in the near surface. The orientation of the NMO ellipse in the near surface has an average of about -30° , relative to the geographic north. This result coincides with the information obtained from geology and near surface studies. This work opens the door for further studies to examine other GPR wave modes and different geologic models. Finally, this study provides important 3-D applications for GPR imaging of the near subsurface, and in inverting for the medium parameters in environmental and near surface problems.

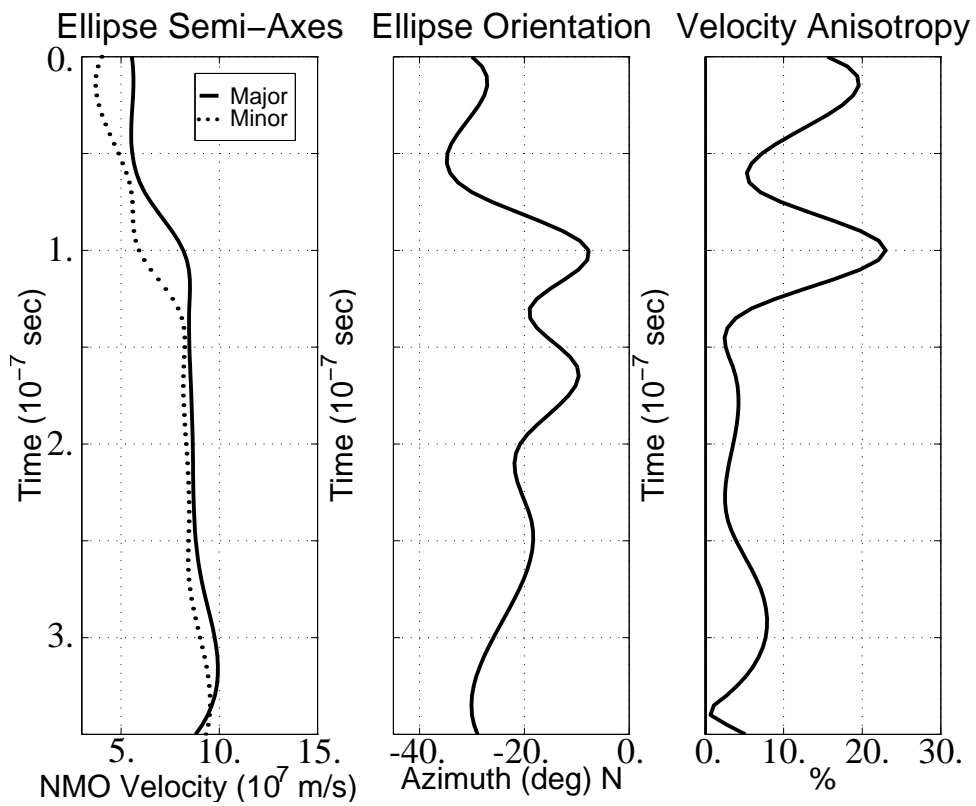


Figure 10: Inversion results as a function of time for (A) the major semi-axis (solid) and the minor semi-axis (dashed) of the NMO ellipse, (B) the orientation of the principal directions relative to the geographic north, and (C) the strength of anisotropy given in percentage.

5 Acknowledgements

We thank Dr. E. Schwatz, DVM, and Indian Echo Caverns for their support. Special thanks to John Grotzinger, Dan Burns, Yervant Vichabian, and John Sogade from the Earth Resources Laboratory (ERL) at the Massachusetts Institute of Technology (MIT) for the useful discussions. We thank the sponsors of the ERL for supporting this study. Al-Dajani would like to acknowledge the financial support from the Saudi Arabian Oil Company (Saudi Aramco).

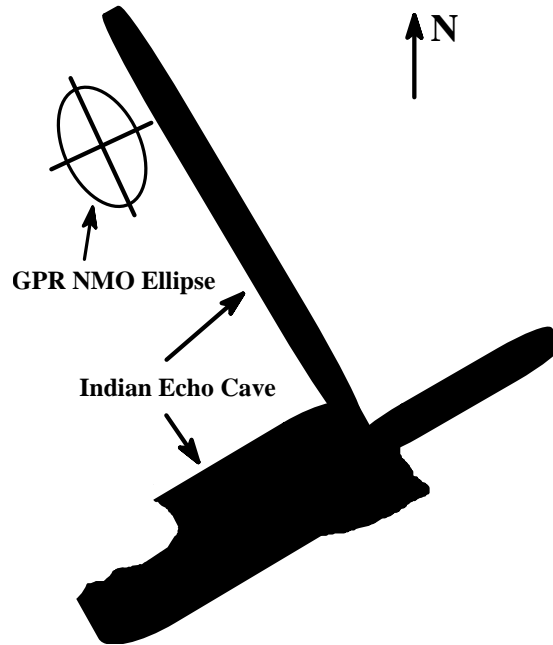


Figure 11: The inverted ellipse superimposed on the cave map. The NMO-velocity ellipse agrees well with the orientation of the cave direction and the local tectonic-induced fracture.

References

- A. Al-Dajani and T. Alkhalifah. Reflection moveout inversion for horizontal transverse isotropy: Accuracy, limitation, and acquisition. *Geophysics*, 65(1):222–231, 2000.
- A. Al-Dajani, T. Alkhalifah, and F. D. Morgan. Reflection moveout inversion in azimuthally anisotropic media: accuracy, limitations, and acquisition. *Geophysical Prospecting*, 47:735–756, 1999.
- A. Al-Dajani and M. N. Toksöz. Nonhyperbolic reflection moveout for azimuthally anisotropic media. Technical report, Earth Resources Laboratory Annual Report, the Massachusetts Institute of Technology, 1999. Also, the 68th Ann. Internat. Mtg, Soc. Expl. Geophys., Expanded Abstracts, 1998, pp. 1497-1482.
- A. Al-Dajani and M. N. Toksöz. Shear-wave reflection moveout for azimuthally anisotropic media. Technical report, Earth Resources Laboratory Annual Report, the Massachusetts Institute of Technology, 2000. Also, the 70th Ann. Internat. Mtg, Soc. Expl. Geophys., Expanded Abstracts.
- A. Al-Dajani and I. Tsvankin. Nonhyperbolic reflection moveout for horizontal transverse isotropy. *Geophysics*, 63(5):1738–1753, 1998.

- T. Alkhalifah and I. Tsvankin. Velocity analysis for transversely isotropic media. *Geophysics*, 60:1550–1566, 1995.
- A. P. Annan and Cosway. Ground penetrating radar survey design. *Symposium on the Application of Geophysics to Engineering and Environmental Problems*, 1992.
- B. A. Auld. *Acoustic Fields and Waves in Solids*. Krieger Publishing Company, Malabar, FL, USA, 1990.
- D. B. Cist. *Ground Penetrating Radar Characterization of Geologic Structure beneath the Aberjona Wetland*. PhD thesis, the Earth Resources Laboratory, Massachusetts Institute of Technology, 1999.
- C. H. Dix. Seismic velocities from surface measurements. *Geophysics*, 20:68–86, 1955.
- V. Grechka and I. Tsvankin. 3-d description of normal moveout in anisotropic inhomogeneous media. *Geophysics*, 63(3):1079–1092, 1998.
- V. Grechka, I. Tsvankin, and J. K. Cohen. Generalized dix equation and modeling of normal moveout in inhomogeneous anisotropic media. 67th Ann. Internat. Mtg., Soc. Expl. Geophys., Expanded Abstracts, 1997.
- H. Hake, K. Helbig, and C. S. Mesdag. Three-term taylor series for $t^2 - x^2$ curves over layered transversely isotropic ground. *Geophysical Prospecting*, 32:828–850, 1984.
- D. Hale, N. R. Hill, and J. Stefani. Imaging salt with turning seismic waves. *Geophysics*, 57:1453–1462, 1992.
- J. A. Kong. *Electromagnetic Theory*. John Wiley and Sons, Inc., New York, NY, USA, 1990.
- D. M. McCann, P. D. Jackson, and P. J. Fenning. Comparison of the seismic and ground probing radar methods in geological surveying. volume 135. IEE Proceedings, 1988.
- P. M. Reppert, F. D. Morgan, and M. N. Toksöz. Gpr velocity determination using brewster angles. pages 455–490. Proceedings of the 7th Inter. Conf. on GPR, 1998.
- P. M. Reppert, F. D. Morgan, and M. N. Toksöz. Ground penetrating radar & avo. SAGEEP, 1999 Conf. Proceedings, 1999.
- O. Yilmaz. *Seismic Data Processing*. Society of Exploration Geophysicists, Tulsa, OK, USA, 1987.